Sensors and Materials, Vol. 26, No. 5 (2014) 279–290
MYU Tokyo

S & M 0992

A Laboratory-Based Three-Phase Smart Grid Sensor Network Testbed

Long-Fung Cheung, King-Shan Lui, Kenneth Kin-Yip Wong, Wing-Kin Lee and Philip Wing-Tat Pong*

Department of Electrical and Electronic Engineering, The University of Hong Kong, Pokfulam Road, Hong Kong Island, Hong Kong

(Received December 24, 2013; accepted March 6, 2014)

Key words: sensor network, smart grid, three phase, testbed, scaled model

A laboratory-based three-phase sensor network testbed for the Smart Grid was developed at the Smart Grid and High-Power System Laboratory of The University of Hong Kong. The setup is featured by a scaled three-phase transmission-line model, visualization of sensor measurement, optical communication network, and integration with global positioning system (GPS). The three-phase transmission-line model consists of three power cables and two transmission towers in which various types of sensors, including magnetic sensors, infrared sensors, strain gauges, and accelerometers, are installed to monitor the condition of the transmission lines and the transmission towers. Magnetic sensors and infrared sensors are employed as advanced sensors, which can provide more accurate and comprehensive information of the transmission line. The sensor data is transferred to a computer for analysis and visualization. A graphical user interface (GUI) was designed in LabVIEW to integrate the data acquisition and display the measurement results, including cable position, inclination and vibration of the tower, and frequency and waveform of the cable current. The host computer also forms an IP network with five remote computers, via optical fibers and an optical interface card, for testing various communication protocols. The topology and connectivity of the network are graphically displayed. The sensor network is integrated with GPS and can perform synchronized measurement with the GPS timing. This sensor network testbed provides a platform for the implementation testing, experimentation, and feasibility evaluation of new sensor applications under test in the Smart Grid.

1. Introduction

The Smart Grid is an idea of modernizing power grids to overcome the existing limitations, shortcomings, and challenges of power systems. Owing to environmental issues, the expansion of transmission grids has been stagnant for decades, which largely constrains the delivery of renewable energy. The ever-increasing cost of fossil fuel

*Corresponding author: e-mail: ppong@eee.hku.hk

is pushing the usage of alternative energy. More and more customers are voicing out the need for transparency and liberty in the power market, high quality/price ratio of electricity, and freedom to interact with the grid. The existing infrastructure is aging, whereas the load demand continues to increase. To prevent a possible decline in reliability, the grid needs to be equipped with the latest technology, such as wide-area measurement and self-healing capability.[1] As a result, many countries are pushing forward the Smart Grid. Slootweg and Enexis[2] define the Smart Grid as a common denominator for a wide range of developments that make medium- and low-voltage grids more intelligent and flexible than they are nowadays. The development of the Smart Grid can improve the utilization of renewable energy, promote the interactive power market, and enhance compatibility and reliability.

Sensors play an important role in making the grid smarter.[3] The Smart Grid will need information more than simply voltage and current. A variety of sensors will be used to detect the environment around the facilities and condition of the infrastructure.[4] Advanced sensors are necessary because of their superior sensitivity, accuracy, and compatibility. Since developmental testing may present an interruption or a reliability threat to a live power system, a testbed for experimenting on various types of sensing technologies and communication protocols in the Smart Grid is needed for testing in an isolated fashion. Gang *et al*. [5] designed a Smart Grid testbed to enable the research community to analyze their designs and protocols in a laboratory environment. Qiu *et al*.[6] built a real-time cognitive radio network for the Smart Grid. Nevertheless, their testbeds do not provide a real transmission model for experiments. To the best of our knowledge, we are the first to develop a testbed for studying three-phase transmission lines in the Smart Grid. Our testbed is designed to perform sensor testing, concept verification, simulation on sensor network,[7] intrasystem communication, and wide-area synchronization.

Our design features a three-phase power transmission system, visualization, multi-sensor network, use of advanced sensors, networking control, and global positioning system (GPS) monitoring. Various types of sensors are employed to provide multiple types of information to the host computer. The uses of optical communication and IP network enhance compatibility and scalability of the setup. The control system processes the sensor data to visualize the transmission line infrastructure and display complicated charts in real time. GPS is deployed to perform synchronization. All the components of this testbed are commercially available, and researchers can build their own setup easily.

2. Testbed Features

2.1 *Platform with multiple advanced sensors*

A complete sensing solution for all the transmission system conditions requires multiple types of sensor.[8] Table 1 shows the responses of the accelerometer, temperature sensor, strain gauge, and magnetic sensor in sagging, tilting, explosion, tower collapse, and electrical fault. Different types of sensors are sensitive to different types of scenarios. For example, an electrical fault can only be sensed by a magnetic field sensor while a tower collapse can be sensed by both a strain sensor and an accelerometer. Therefore, a sensor network with multiple types of sensors is essential

Table 1
(Color online) Sensor response on various events.

	Strain sensor	Accelerometer (Vibration)	Accelerometer (Tilting)	Temperature sensor	Magnetic sensor
Normal	Normal	Normal	Normal	Normal	Normal
Sagging	Increase	Normal	Normal	Increase	Change in magnetic field waveform or distribution
Galloping	Increase	Low frequency, high amplitude	Oscillating	Normal	
Explosion	Increase	Sharp increase	Oscillating	Temporary increase	
Collapse	Sharp increase, then zero	No information	Appreciable tilt 0–90°	No information	
Electrical fault	No information	No information	No information	No information	

for the comprehensive monitoring of transmission lines. Our setup includes a multi-sensor network consisting of strain gauges, accelerometers, infrared sensors, and magnetic sensors. The advanced magnetic sensing technology is adopted because a magnetic sensor is sensitive to all types of abnormal events. As shown in Table 1, the magnetic field waveform and distribution are sensitive to sagging, galloping, explosion, collapse, and electrical fault. Thus, the magnetic field can signify these abnormal events. Owing to its extensive sensing ability, it can be used as a universal sensor. In addition, the magnetic field measured using the magnetic sensor can be used to determine the cable position and perform power quality analysis, which is difficult to achieve using conventional sensors. The advanced temperature sensing technology is also applied in the setup. The infrared sensor can measure the cable temperature without physical contact with a high-voltage cable, which makes installation and maintenance easier and safer. Furthermore, it is equipped with a laser tracking device to measure the temperature of a galloping cable.

2.2 *Visualization of measurement information*

Visualization of measurement information is a key component of the setup because it conveys abstract information in intuitive ways and thus enables users to perceive and understand a large amount of information instantaneously.[9] The monitoring part of our setup is highly visualized to enhance situational awareness and reduce cognitive demand on the operators. The graphical user interface (GUI) displays the measurement and analysis results of the electrical and spatial information of a transmission line and transmission towers in the forms of images, diagrams, and charts. The magnetic field waveform is presented in graphs while the power quality analysis calculated by performing Fourier transform on the magnetic waveform is presented in a spectrum.

2.3 *Integration with GPS*

Our setup is integrated with GPS for providing position and time. As a result, the synchronization accuracy of the sensor network can be boosted from 1 ms up to 1 μs, which is 1000 times better than the current standard.[10] The time provided by the GPS

enables time synchronization for wide-area measurement. The geographical coordinates obtained from the GPS can be fed to Google Earth to provide a satellite aerial map of the sensor network location in the GUI.

3. Hardware Architecture

3.1 *Three-phase three-cable transmission lines, sensors, and electrical system*

The laboratory setup of the testbed is established in the Smart Grid and High-Power System Laboratory at The University of Hong Kong. In this three-phase three-cable power transmission system, the positions of sensors and the GUI are the same for each cable. Figure 1(a) shows a schematic structural diagram of the three-phase transmission lines. The sensor network includes several types of sensors: magnetic sensors, infrared sensors, strain gauges, and accelerometers [Fig. 1(b)]. Each end of the transmission line is installed with one set of strain gauges and one accelerometer. Another accelerometer is mounted on each tower. An infrared sensor is placed 0.15 m horizontally from the transmission line. The distance between towers is 3 m and the ends of the cables are suspended on the towers 1 m from the ground, and the separation between adjacent cables is 200 mm. Each cable is connected to each phase of the three-phase 50 Hz mains power supply. Figure 2 shows a schematic diagram of the electrical connection of this three-phase power transmission system. Sensors are installed on the three-phase power transmission lines suspended by the two transmission towers. The three-phase power cables are connected to the power switch via a three-phase connector. The phase separation among the three phases is 120°. The power switch is connected to the mains switch box via the Neutral Line and Ground Line. A miniature circuit breaker (MCB) protects the circuit from damage caused by overloading or short circuit.[11] The MCB can be reset to resume normal operation after a faulty condition. A residual-current device (RCD) protects users from electric shock owing to electricity leakage.[12] MCB and

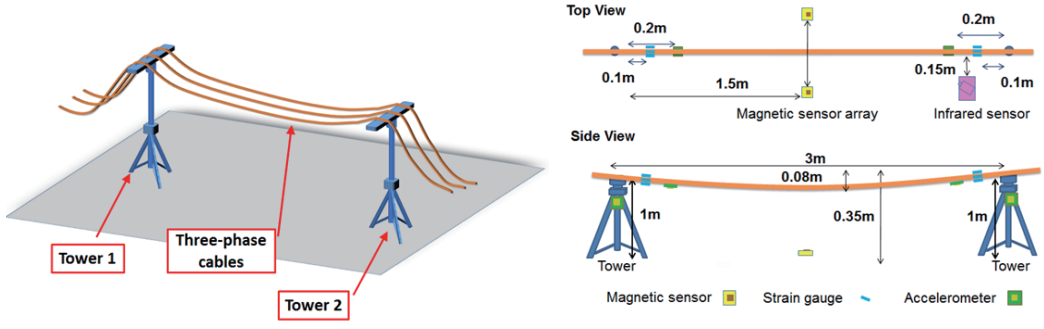

(a) (b)

Fig. 1. (Color online) Schematic diagram of three-phase power transmission system. (a) Three-phase cables are suspended by two transmission towers. (b) Positions of the towers, power cables, magnetic sensor array, strain gauges, accelerometers, and infrared sensor.

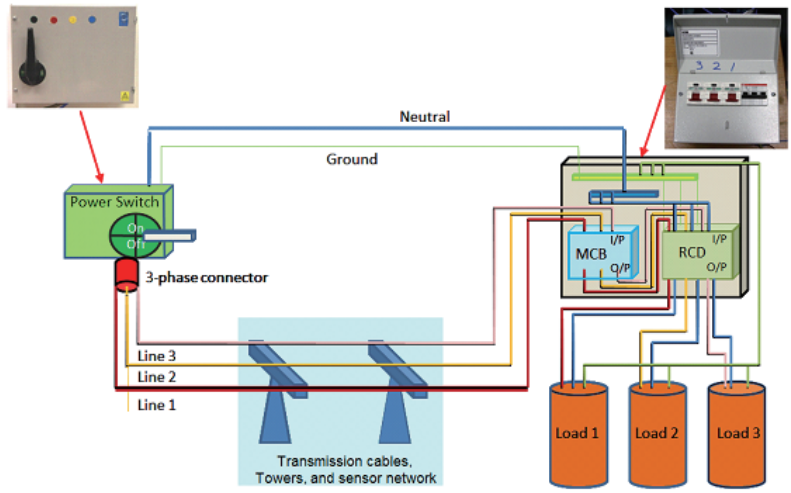

Fig. 2. (Color online) Schematic diagram of electrical connection of three-phase power transmission system. Photos of power switch and mains switch box are shown.

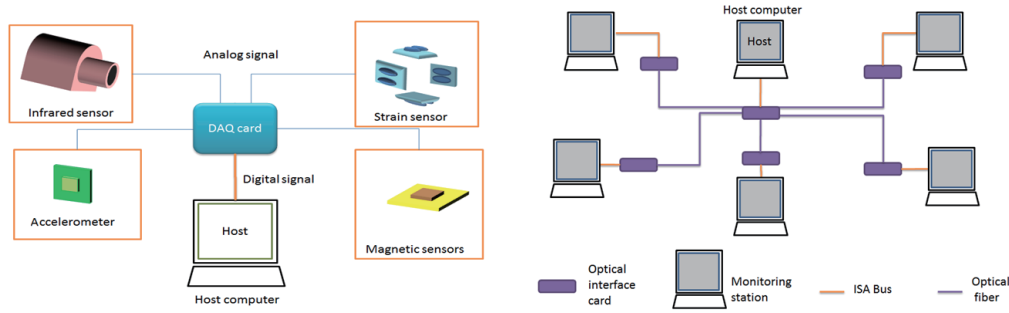

(a) (b)

Fig. 3. (Color online) (a) Illustration of sensor network. Sensors are connected to a computer via a DAQ card. (b) Illustration of monitoring station network. Host computer is connected to five other monitoring station computers via optical link.

RCD are used together to enhance safety. The rated voltage and power for the loading of each phase line are 220–240 V and 1850–2200 W, respectively. The other side of each loading is connected to the Earth and Live Line.

3.2 *Sensor data transmission and network connection*

A data-acquisition (DAQ) card (National Instruments NI USB 6211 M) establishes a link between the host computer (monitoring station) and the sensors [Fig. 3(a)]. It

collects the analog data from the sensors, converts them into digital form, and sends them via a USB hub to the host computer, which plays the role of a monitoring station that analyzes the information from sensors and monitors the transmission line. There are 16 analog input channels with ±10 V voltage range (16 bits) with a high sampling rate of 250k samples per second. To provide a platform for testing and implementing communication protocols, there are five computers simulating other monitoring stations and they are connected with the actual monitoring station by optical communication links. Figure 3(b) shows the schematic diagram of this monitoring station network. Between the host and each of the other five monitoring stations, there are optical fibers and optical interface cards (OLYCOM OM910-FE/S25). The optical interface cards convert digital signals into optical signals to be conveyed by the optical fibers. These interface cards are capable of operating at 100 Mbps, providing a network throughput of 200 Mbps in full-duplex mode. The single-mode optical fibers are connected to the optical interface cards with the FC/PC connectors.

3.3 *Testbed characterization and performance in operation*

The operation of this three-phase transmission-line model was characterized using a 3-phase power quality analyzer (Fluke 434). The phase current in one phase line can be varied from 0 to 43 A (Fig. 4) without affecting the others (Fig. 5). The phase separation of 120° can be observed from Fig. 5(d).

The GUI of the monitoring station is shown in Fig. 6. The diagram labeled by (1) is the position chart indicating the position of the mid-span of the transmission line. The position is derived from the magnetic field measured by two magnetic sensors based

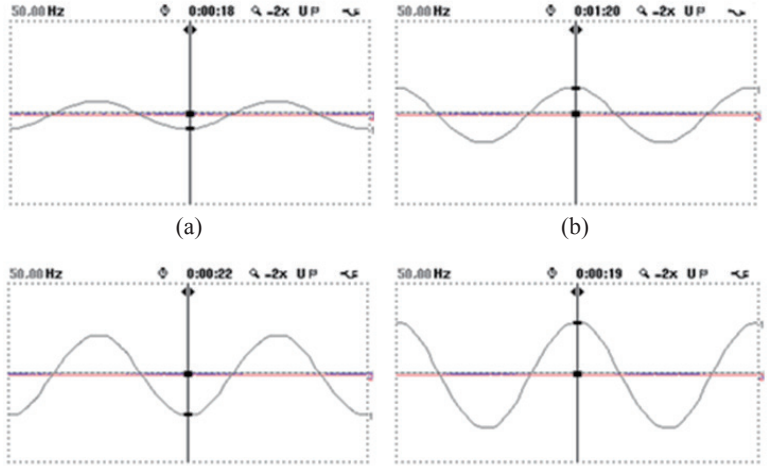

Fig. 4. (Color online) Electrical current flowing in each phase conductor in the three-phase transmission-line model measured using a power quality analyzer. (a) Phase A current = 12 A, Phase B current = 0 A, Phase C current = 0 A. (b) Phase A current = 22 A, Phase B current = 0 A, Phase C current = 0 A. (c) Phase A current = 34 A, Phase B current = 0 A, Phase C current = 0 A. (d) Phase A current = 43 A, Phase B current = 0 A, Phase C current = 0 A. The electrical current in each phase conductor can be varied from 0, 12, 22, and 34 A to 43 A.

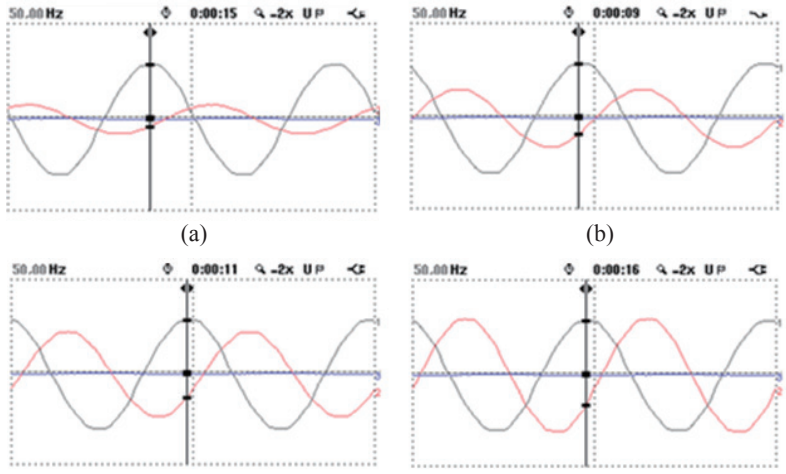

Fig. 5. (Color online) Electrical current flowing in each phase conductor in the three-phase transmission-line model measured using a power quality analyzer. (a) Phase A current = 43 A, Phase B current = 12 A, Phase C current = 0 A. (b) Phase A current = 43 A, Phase B current = 22 A, Phase C current = 0 A. (c) Phase A current = 43 A, Phase B current = 34 A, Phase C current = 0 A. (d) Phase A current = 43 A, Phase B current = 43 A, Phase C current = 0 A. The variation of electrical current in one of the phase conductors does not affect the others.

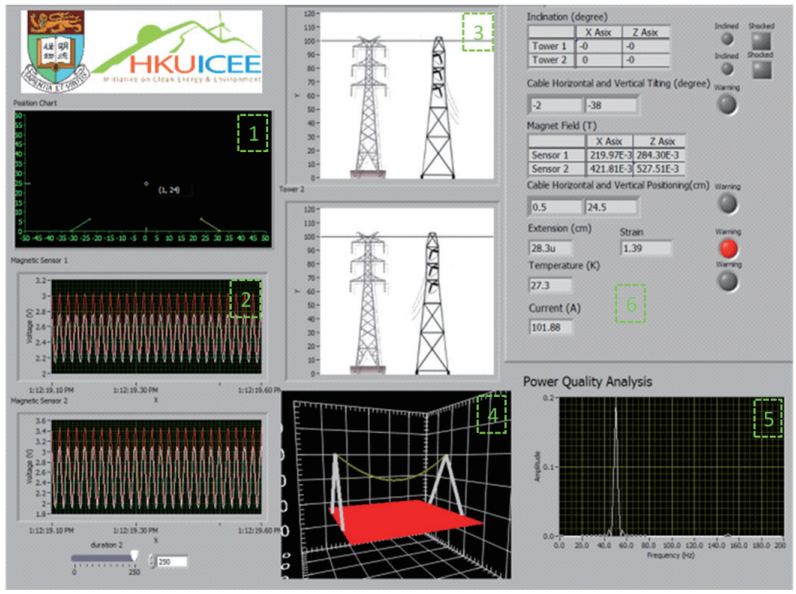

Fig. 6. (Color online) GUI of the monitoring station. The interface includes (1) position chart, (2) magnetic field waveform, (3) inclinations of Towers 1 and 2, (4) three-dimensional monitoring of the transmission line, (5) power quality analysis spectrum, and (6) numerical measurement information panel. The setup is sponsored by the Initiative on Clean Energy and Environment of The University of Hong Kong (HKUICEE), which is displayed in the upper left corner.

on the Biot-Savart Law. The performance of the magnetic sensors was evaluated for the scenarios of sagging and galloping of one of the cables. The position of the cable before and after sagging or galloping can be determined accurately with an error of less than 5%, as one can observe from Figs. 7 and 8, respectively. As the transmission line is monitored using two magnetic sensors, there are two magnetic waveforms displayed in the graphs labeled by (2) in Fig. 6. The magnetic waveforms are essentially the waveforms of the electrical currents in the transmission lines as governed by the Biot-Savart Law. The inclination diagrams (3) show the front and side views of Towers 1 and 2 and users can observe if there is any inclination for the transmission towers. The inclination is calculated from the tilting angles measured using the accelerometers

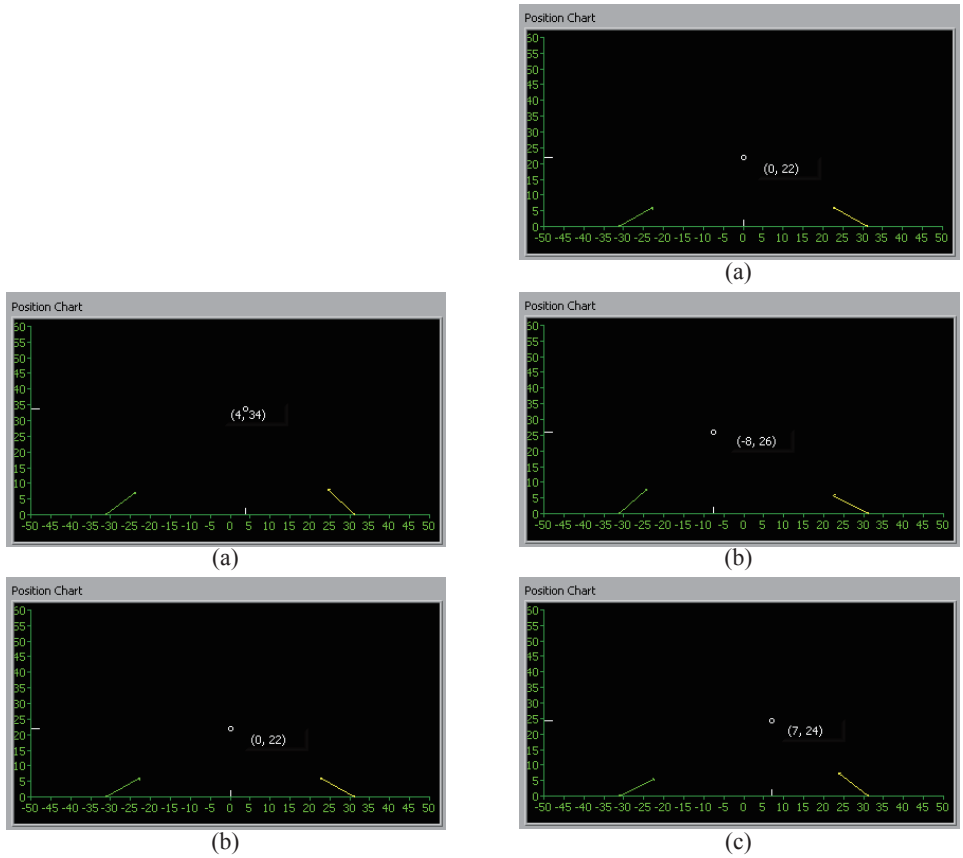

Fig. 7 (left). (Color online) Position of one of the phase conductors carrying electrical current (the other two conductors are not carrying current) (a) before and (a) after sagging. The white dots indicate the conductor position. The level of the dot in (a) is higher than that in (b). This matches with the result of sagging. The unit for the *x*- and *y*-axes is cm.

Fig. 8 (right). (Color online) Position of one of the phase conductors carrying electrical current (the other two conductors are not carrying current) (a) before and (b)(c) during galloping. The white dots indicate the conductor position. (b) shows the conductor position swinging to the left while (c) shows the conductor position swinging to the right. The unit for the *x*- and *y*-axes is cm.

mounted on the transmission towers. The tower inclination was tested as shown in Fig. 9. The test result shows that the inclination graph can well reflect the tower tilting. Diagram (4) is the three-dimensional monitoring of the transmission line derived from the tilting angles measured using the accelerometers mounted on the transmission line. The catenary of the cable before and after sagging can be observed in real-time with this 3D diagram (Fig. 10). Spectrum (5) is the power quality analysis by taking the Fourier transform with the magnetic field waveform measured using the magnetic sensors as shown in (2). The GUI also provides numerical measurement information in the panel labeled by (6). The numerical information includes the cable temperature measured using the infrared sensor, cable tension measured using the strain gauges, magnitude of the electric current carried by the transmission line as determined by inverse calculation from the magnetic field measured using the two magnetic sensors, and the exact values of the tower inclinations. If these values exceed certain predetermined safety levels,

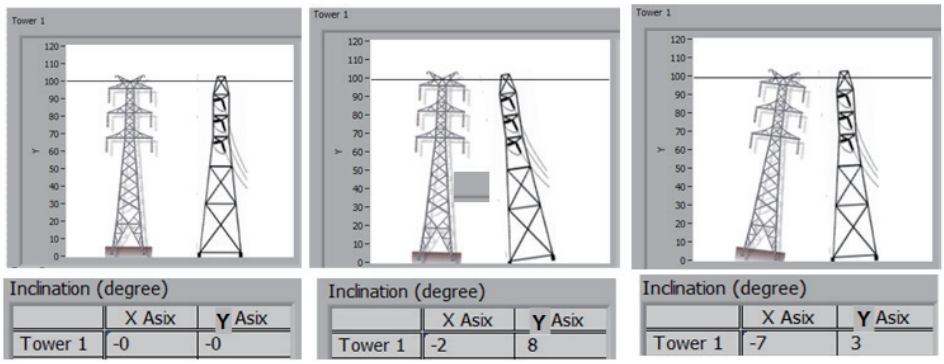

(a) (b) (c)

Fig. 9. (Color online) Inclination of transmission tower monitored by accelerometers. (a) shows transmission tower without inclination; the inclination reading (deg) in *x*- and *y*-axes is (0, 0). (b) shows transmission tower inclining along *y*-axis; the inclination reading is (–2, 8); (c) shows transmission tower inclining along *x*-axis; the inclination reading is (–7, 3).

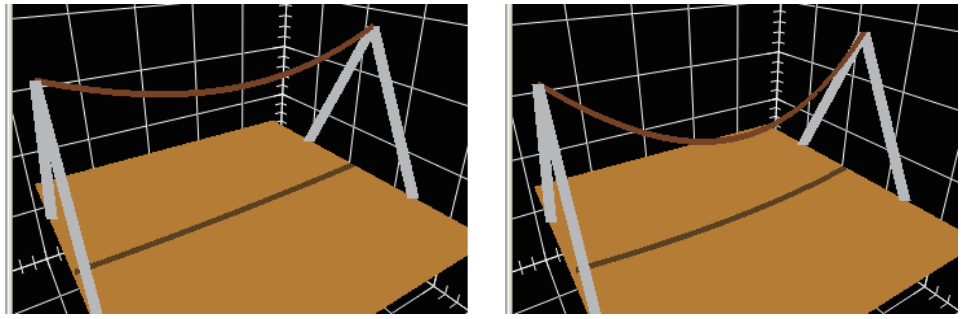

(a) (b)

Fig. 10. (Color online) Accelerometers providing 3D monitoring of transmission line. (a) shows the transmission line before sagging, whereas (b) shows the transmission line after sagging. The brown line is the transmission line. The catenary of the cable changes owing to sagging.

the corresponding warning indicators are lit up to alert the operators. When there is strong vibration to the tower owing to, for example, explosion by terrorist sabotage, the oscillation is sensed by the accelerometers mounted on the transmission towers and the corresponding "Shocked" indicator is lit up to alarm the operators. As such, all the abnormal events listed in Table 1 can be effectively monitored in this sensor network testbed.

As discussed earlier, this testbed is equipped with the features of networking control and GPS monitoring. In the setup, the host computer is connected to five remote computers via optical fibers. The network is visualized in the interface of the host computer (Fig. 11). The network can be rearranged from the star configuration to another configuration that suits the need of any experiments and simulations. The interface can also be integrated with various protocols to perform synchronization, protective relaying, etc. The IP address and connection status of each computer are shown in the interface. The interface could correctly indicate the network activity in the testing. The GPS monitoring is performed in another interface (Fig. 12). The map obtained from Google Earth correctly shows the geographical location of the testbed with accuracy within 2.2 m. The GPS of the system can track satellites in parallel with twenty channels for acquisition (1 s for hot start), reacquisition (0.1 s average), and synchronization (1 μs).

4. Conclusions

The laboratory-based three-phase transmission-line sensor network testbed is featured using a platform with multiple advanced sensors, a GUI visualizing the measurement information, and integration with GPS. The monitoring station has access to all the sensor data and it can carry out further analysis to provide monitoring of the transmission

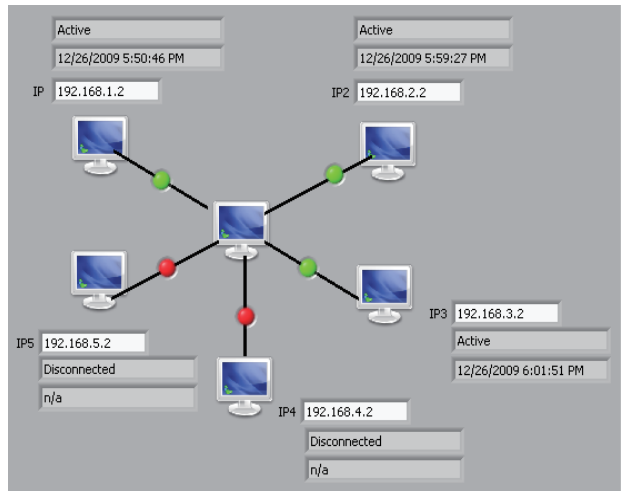

Fig. 11. (Color online) Networking control interface. IP address and connection status of each computer are shown.

Fig. 12. (Color online) GPS monitoring interface. The latitude and longitude of the testbed are acquired using the GPS. These data are sent to Google Earth to obtain the aerial location map. The location shown is the Smart Grid and High-Power System Laboratory of The University of Hong Kong. GPS timing is displayed at the top.

line. The system can detect various electrical and spatial abnormal events of the transmission line, including cable sagging and galloping, tower collapse and explosion, and electrical faults. Moreover, it is equipped with a GPS receiver and can perform time synchronization for wide-area measurement. The performance of the testbed was tested and verified in this work. Compared with the other Smart Grid testbed systems that focus on energy flow[5] and communication,[6] this setup offers the unique advantage that it was particularly designed for implementing sensor networks on transmission grids. It provides a three-phase transmission-line model for experimenting on various sensor network facilities in Smart Grid research, for example, synchronized wide-area measurement. It is a comprehensive platform for experimenting on various sensor network schemes and protocols for the Smart Grid. On the basis of this Smart Grid testbed, two scientific works have already been carried out and published.[13,14]

Acknowledgements

This work was supported in part by the Seed Funding Program for Basic Research, Small Project Funding Program, and Initiatives on Clean Energy and Environment from The University of Hong Kong, ITF Tier 3 funding (ITS/112/12), RGC-GRF grant (HKU 704911P), and University Grants Committee of Hong Kong (Contract No. AoE/P-04/08).

References

1 X. S. Zhou, L. Q. Cui and Y. J. Ma: Int. Conf. on Computer Application and System Modeling, 2010, Vol. 3, pp. 599–603.
2 H. Slootweg and B. V. Enexis: IET Smart Metering – Making It Happen, 2009, pp. 1–9.
3 Y. Yang, F. Lambert and D. Divan: IEEE Power Engineering Society General Meeting, 2007, pp. 1–8.
4 R. A. Leon, V. Vittal and G. Manimaran: IEEE Trans. Power Delivery **22** (2007) 1021.
5 L. Gang, D. De and W. Z. Song: 1st IEEE Int. Conf. on Smart Grid Communications, 2010, pp. 143–148.
6 R. C. Qiu, Z. Chen, N. Guo, Y. Song, P. Zhang, H. Li and L. Lai: 5th IEEE Workshop on Networking Technologies for Software Defined Radio Networks, 2010, pp. 1–6.
7 Y. C. Lee, H. Y. Lai and P. J. Lee: IJETI **2** (2012) 283.
8 R. K. Aggarwal, A. T. Johns, J. A. S. B. Jayasinghe and W. Su: Electr. Power Syst. Res. **53** (2000) 15.
9 B. Xu, C. Yuksel, A. Abur and E. Akleman: IEEE Electrotechnical Conf., 2006, pp. 943–947.
10 M. T. S. van As and H. J. Vermeulen: IEEE Africon Conference in Africa, 2002, vol. 2, pp. 853–857.
11 Y. Y. Luo, J. G. Lu and Z. G. Li: Proc. 58th IEEE Holm Conference on Electrical Contacts, 2002, pp. 80–85.
12 M. Mitolo: IEEE Trans. Ind. Appl. **46** (2010) 1552.
13 X. Sun, Q. Huang, Y. Hou, L. J. Jiang and P. W. T. Pong: IEEE Trans. Power Delivery **28** (2013) 2145.
14 X. Sun, K. S. Lui, K. K. Y. Wong, W. K. Lee, Y. Hou, Q. Huang and P. W. T. Pong: IEEE Trans. Magn. **47** (2011) 2608.